



UNIVERSITAT
JAUME·I

Technical Report ICC 2013-03-01

Concurrent and Accurate RNA Sequencing on Multicore Platforms

Héctor Martínez^{*}, Joaquín Tárraga[†], Ignacio Medina[†], Sergio Barrachina^{*},
Maribel Castillo^{*}, Joaquín Dopazo[†], Enrique S. Quintana-Ortí^{*}

^{*}Dpto. de Ingeniería y Ciencia de los Computadores
Universidad Jaume I
12006 - Castellón
Spain
{martineh,barrachi,castillo,quintana}@uji.es

[†]Computational Genomics Institute
Centro de Investigación Príncipe Felipe
46012 - Valencia
Spain
{jtarraga,imedina,jdopazo}@cipf.es

February 25, 2022

Concurrent and Accurate RNA Sequencing on Multicore Platforms

Héctor Martínez* Joaquín Tárraga† Ignacio Medina† Sergio Barrachina*
Maribel Castillo* Joaquín Dopazo† Enrique S. Quintana-Ortí*

February 25, 2022

Abstract

In this paper we introduce a novel parallel pipeline for fast and accurate mapping of RNA sequences on servers equipped with multicore processors. Our software, named **HPG-aligner**¹, leverages the speed of the Burrows-Wheeler Transform to map a large number of RNA fragments (reads) rapidly, as well as the accuracy of the Smith-Waterman algorithm, that is employed to deal with conflictive reads. The aligner is complemented with a careful strategy to detect splice junctions based on the division of RNA reads into short segments (or seeds), which are then mapped onto a number of candidate alignment locations, providing useful information for the successful alignment of the complete reads.

Experimental results on platforms with AMD and Intel multicore processors report the remarkable parallel performance of **HPG-aligner**, on short and long RNA reads, which excels in both execution time and sensitivity to an state-of-the-art aligner such as TopHat 2 built on top of Bowtie and Bowtie 2.

Keywords: RNA, Short-read alignment, Burrows-Wheeler Transform, Smith-Waterman’s Algorithm, high performance computing, multicore processors.

1 Introduction

Over the last few years, biology has experienced a revolution as the result of the introduction of new DNA sequencing technology, known as Next-Generation Sequencing (NGS), that nowadays makes it possible to sequence the genomic DNA or RNA transcripts, or transcriptome, in a few days instead of years, at a very low cost. These recent high-throughput sequencers produce data at unprecedented rates and scale, with associated sequencing costs in continuous decrease. In particular, RNA sequencing (RNA-seq) technology [1] has arisen as a crucial analysis tool for biological and clinical research, as it can help to determine and quantify the expression of genes, the RNA transcripts, that are activated or repressed as the result of different diseases or phenotypes, therefore providing an unbiased profile of a transcriptome that helps to understand the etiology of a disease. In consequence, RNA-seq is increasingly replacing conventional expression microarrays in most practical scenarios [1].

Current NGS technology can sequence short DNA or RNA fragments, of length usually between 50 and 400 nucleotides (nts), though new sequencers with longer fragment sizes are being developed. Primary data produced

by NGS sequencers consists of hundreds of millions or even billions of short DNA or RNA fragments which are called reads. The first step in NGS data processing in many comparative genomics experiments, including RNA-seq or genome resequencing [2], involves mapping the reads onto a reference genome, in order to locate the genomic coordinates where these fragments come from. This step constitutes an extremely expensive process from the computational point of view. Furthermore, sensitivity is also a serious concern at this point [3], given that natural variations or error sequencing may occur, yielding frequent mismatches between reads and the reference genome, which increase the computational complexity of the procedure.

The mapping process is particularly more difficult for RNA-seq, as the genes in eukariotes may be split into small regions, called exons, that are separated by intron zones composed of thousands of nucleotides. Once the exons are transcribed to RNA, they are brought together to form the transcripts in a splicing process. Thus, when mapping reads from RNA transcripts onto a reference genome, it must be taken into account that these reads may contain a splice junction and, therefore, involve different exons, so that in practice they may lie thousands of nucleotides apart. This situation is referred to as a gapped alignment.

Recently, a variety of programs based on the Burrows-Wheeler Transform (BWT) [4] have been developed with the goal of accelerating the mapping process [5, 6]. BWT is a popular pruning technique that has been successfully applied to accelerate ungapped alignment in genome index-based searches. A strategy that combines index-based read mapping with splice junction detection has been imple-

*Dpto. de Ingeniería y Ciencia de los Computadores, Universidad Jaume I, 12006 - Castellón, Spain.

{martineh,barrachi,castillo,quintana}@uji.es

†Computational Genomics Institute, Centro de Investigación Príncipe Felipe, 46012 - Valencia, Spain.

{jtarraga,imedina,jdopazo}@cipf.es

¹HPG-aligner is an open-source software application. It can be downloaded from <http://www.opencb.org/>.

mented in TopHat [7], a software package that is extensively used for the analysis of RNA-seq experiments. TopHat internally invokes Bowtie [2], a program for read mapping but with no support for gapped alignment. To tackle this in TopHat, read mappings that lie in close genomic locations are combined to reconstruct putative exon junctions, where unmapped reads are tried again. However, this approach presents performance and sensitivity problems, rooted in the *ad hoc* junction detection algorithm and the read mapping. The underlying reason is basically that Bowtie only permits a small number of mismatches, which are insufficient for the current dimension of reads, therefore failing to map a large number of reads. Although Bowtie 2 [8] significantly accelerates the mapping step, the strategy for junction detection remains unchanged in TopHat.

In this paper we contribute an innovative strategy that combines an efficient algorithm for junction detection and a mapping algorithm with notably improved sensitivity that correctly aligns reads with a high rate of mutations (errors), insertions or deletions (EIDs). This strategy, implemented as a parallel pipeline in a program called HPG-aligner, shows excellent sensitivity and remarkable parallel performance for both short and long RNA-seq reads, presenting runtimes that linearly depend on the number and the length of reads. In HPG-aligner, reads are aligned using a combination of mapping with BWT and local alignment with the Smith-Waterman algorithm (SWA) [9]. As BWT is faster but less precise than SWA, we employ the former in the early stages of the process, to obtain a rapid mapping of a large number of reads (those which contain few EIDs); on the other hand, SWA is applied in the final stages, to reliably map conflictive reads. Furthermore, in our approach splice junctions are detected by dividing unmapped reads into multiple seeds, which are next mapped using BWT at distances compatible with the length of an intron. The potential mapping regions detected using these seeds are then identified and brought together to perform SWA alignment.

The rest of the paper is structured as follows. In section 2 we describe the pipelined organization of HPG-aligner and the operation of the different stages. In section 3 we review the parallelization of the pipeline using OpenMP, a standard for portable shared memory parallel programming [10]. A detailed experimentation is reported next, in section 4, exploring the performance of the stages and the full pipeline from the perspective of both parallelism and scalability on a server equipped with 64 AMD cores; moreover, in that section we also include a comparison of HPG-aligner against TopHat 2 on a platform with 12 Intel cores. We finally close the paper with a discussion of conclusions and future work in section 5.

2 The Mapping Pipeline

The HPG-aligner pipeline maps RNA sequences into the reference genome, with the mapping process being divided into the stages *A–F* illustrated in Figure 1. The interaction between two consecutive stages follows the well-known producer-consumer relation, and is synchronized through a shared data structure, where the producer inserts work

for the consumer to process. In the following paragraphs we discuss the tasks performed in each one of these stages together with relevant algorithmic details. We note that three of the pipeline stages (*B*, *C* and *E*) heavily rely on BWT and SWA.

2.1 Stage A: Read Data

Initially the data corresponding to the RNA reads are stored in a disk file following the standard FASTQ format [11]. Due to the large number of reads involved per experiment (typically, dozens of millions) and the information that needs to be maintained per read, this file is quite big, and in general exceeds the capacity of the main memory. (Although the file sizes can vary much depending on the case study, in our experiments we often had to deal with files of 40–50 GBytes, which obviously will not fit in the memory of most of today’s desktop servers.)

Therefore the principal task of this stage consists in retrieving data from the disk in blocks, hereafter referred to as *batches of reads*, with about 200 reads per batch, that are then stored in the *Read queue* for latter consumption by the subsequent stage. The batches of reads are kept in main memory in an array list, which accommodates fast serial and indexed access. Among other information, this array records the header, sequence, size, and quality of each read.

2.2 Stage B: BWT

This stage performs a fast mapping of reads to the genome, using our own implementation of the BWT. The procedure extracts a batch from the read queue, and then applies the BWT-based algorithm, allowing up to 1 EID per read.

If the read is successfully mapped, this stage creates an *alignment record* for each mapping that identifies the chromosome, among other information, with the initial and final positions of the read within the chromosome, and the strand. Otherwise, the information that identifies the unmapped read is stored in a *target array*. The alignment records and target array conform a single data structure with the batch of reads, that is passed to the next stage once all the reads of the batch have been processed, via the *BWT queue* (which contain both mapped and unmapped reads).

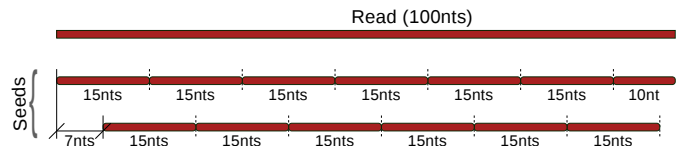


Figure 2: A read split into multiple overlapping seeds.

2.3 Stage C: Region Seeker

Given a batch in the BWT queue, this stage only processes the unmapped reads, leaving untouched those reads that were already mapped in the previous stage. Each unmapped read of the batch is split in this stage into a number of overlapping “fragments”, hereafter referred to as

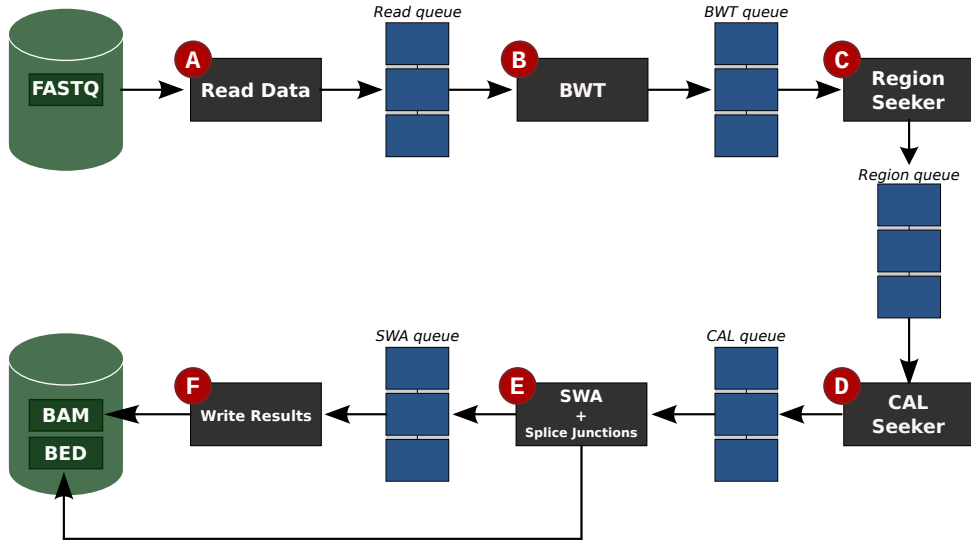


Figure 1: Pipelined organization of the RNA mapper.

seeds, tentatively of 15 nts each. For example, given a read comprising 100 nts, 15 overlapping seeds can be obtained: 8 seeds by starting the splitting at the first nucleotide of the read, and 7 seeds more by starting the splitting at the eight nucleotide of the read (see Figure 2).

Next, the BWT-based algorithm is employed again to map each one of these seeds into the reference genome, though this time no EIDs are permitted. The rationale of this process is the following. The most likely reason a given read was not mapped in stage *B* is that it contained more than one EID. By dividing the read into shorter seeds, we expect that all the EIDs of the read are concentrated in only a few of these seeds. Therefore, the majority of the seeds will be successfully mapped into the reference genome with no EIDs.

Note that the seeds are quite small, leading to a new problem as it is now very likely that each seed will be mapped to more than one place in the reference genome. The result of mapping these seeds is therefore a large collection of what we call *regions*, which identify all the places in the reference genome where these seeds were successfully mapped.

Once the full batch of reads is processed, the results are stored as part of the same data structure and passed to the next stage via the *Region queue*.

2.4 Stage D: CAL Seeker

This stage also processes the input information by batches, skipping the reads that were already mapped in stage *B*. For each unmapped read in the batch, this stage uses the regions produced by stage *C* to obtain a list of *candidate alignment locations* (CALs), which define potential mappings of that read.

Let us briefly elaborate on this. As stated previously, for each read, the previous stage will have likely detected a considerable number of regions due to the multiple matchings of the corresponding individual seeds. Nevertheless, we expect than only those regions that are related to a correct mapping of the read lie close together. We consider

these areas as potential mappings of some part of the read, and therefore we identify them as CALs.

In particular, to obtain the CALs for a given read, this stage first merges the regions of one read that are less than a certain number of nucleotides apart; and then classifies each merged region as a CAL only if its number of nucleotides is larger than a given threshold. Figure 3 shows two CALs, CAL_0 and CAL_1 , that have been identified from the regions obtained by mapping the seeds of a given read. In this figure, the gaps in the regions represent the places where some of the seeds could not be properly matched to the reference genome.

At the end of this stage, the CALs are recorded in a data structure which is passed to the next stage via the *CAL queue*. Furthermore, to save space, the information about the regions is deleted at this point, as it will not be used in subsequent stages.

2.5 Stage E: SWA + Splice Junctions

This stage performs five consecutive tasks: i) CALs are extended with additional information from the reference genome; ii) extended CALs which are close to each other in the reference genome are joined; iii) the current read is mapped onto all extended CALs (joined or not), using our implementation of SWA; iv) successful mappings are recorded into a data structure and splice junctions are detected; and, finally, v) splice junctions are written to disk. The following paragraphs describe these five tasks in more detail.

The first task extends the CALs in order to include fragments from the reference genome that help to completely align a read. The CALs of a read are extended to both left and right by a fixed number of nucleotides (30 nts by default), though this could lead to intron fragments being included in the extended CALs. This process is graphically illustrated in the upper part of Figure 4.

The second task connects extended CALs which are close to each other in the reference genome. All the extended CALs whose distance to each other is shorter than the

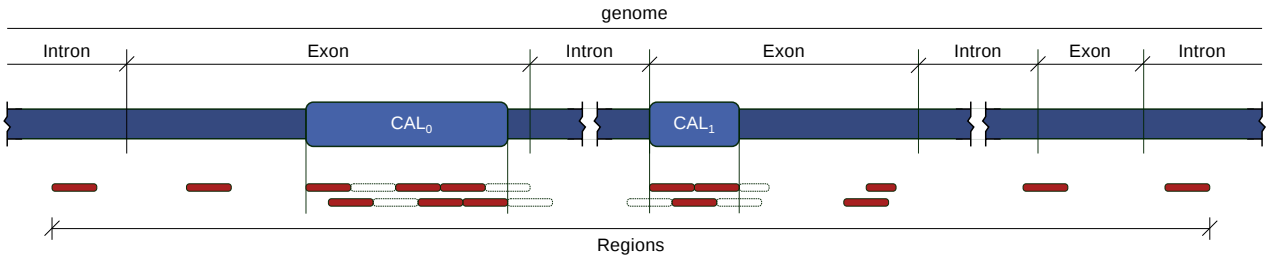


Figure 3: Identification of CALs from regions.

longest known intron are merged, generating a *joined extended CAL*; see Figure 4. Note that joined extended CALs involving more than two CALs are also possible.

After these two tasks, we will have identified a collection of extended CALs and joined extended CALs, which are potential mapping candidates for the given read. The following task maps the read onto all of these, employing our own implementation of SWA. This task returns the alignment between the read and each extended CAL, the statistics of the alignment (e.g., quality score), and the initial position of the alignment.

The fourth task is only performed on those SWA alignments with alignment scores above a given threshold, that indicates a successful mapping. In those cases, this task creates an alignment record that identifies the chromosome, the initial and final positions of the read within the chromosome, the strand, etc. These alignment records are passed to the next stage via the *SWA queue*.

This fourth task also searches for splice junctions. For this purpose, a large number of consecutive deletions in the alignment returned by SWA is used as an indication of a potential splice junction; see Figure 5. We expect that these deletions are due to the intron fragments that were included in the joined reference when the CALs were extended. Therefore, to assess if a large gap is an actual splice junction, the start and end marks of an intron are searched for the specific nucleotide sequences “GT-AG” and “CT-AC”.

All the splice junctions and the number of times each of them has been detected are written to disk when the batches are processed. Therefore, this information must be maintained and updated during the whole process (i.e., not only for the current batch). To reduce the memory space needed to hold the information on detected splice junctions, as well as to rapidly find whether the last detected splice junction was previously detected, a self-balancing binary search tree (an AVL tree) data structure is used to hold this information.

The last task of this stage simply writes the detected splice junctions to an output file on disk, with the BED format [12]. As stated before, this information is written to disk only when the last batch has been processed.

2.6 Stage *F*: Write Results

This stage completes the processing of a read batch, writing to disk whether each read was mapped or not, following the BAM format [13]. The output file contains, among other information, the read id (the first component of the

header), the sequence, and its quality. In addition, whether the current read was mapped, the chromosome, and the initial position are also written to the output file.

3 Leveraging Inter-stage and Intra-stage Concurrency

The pipelined organization of our HPG-aligner mapper naturally accommodates two types of algorithmic concurrency, both targeting the hardware parallelism of current multi-core processors. On one side, the mapper is divided into a number of independent stages, connected via queues that act as data buffers and synchronize the relative processing speeds (throughput) of consecutive stages. Provided each one of these stages is run on a separate thread and a different (CPU) core, the result is an overlapped execution of the stages —see the execution trace in Figure 6 (top)—, much like the exploitation of instruction-level parallelism that occurs in a pipelined processor [14]. The actual benefits that this pipelined organization yields, in terms of reduced execution time, are experimentally analyzed in the next section.

On the other side, in case there exists a sufficient number of computational resources (basically, cores), nothing prevents our scheme from also leveraging the concurrency intrinsic to each one of the stages, so that more than one thread can operate per stage, mimicking the operation of a pipelined superscalar processor [14]; see the execution trace in Figure 6 (bottom). The purpose of exploiting intra-stage concurrency is to both accelerate and equilibrate the processing speeds of the different stages, as the throughput of the full pipeline is dictated by the performance of the slowest stage.

We next discuss the general parallel pipelined framework as well as the specific approaches that were adopted in our scheme to exploit concurrency within stages *B–E*. Stages *A* and *F* both perform I/O from/to the disk and, thus, there is not much to be gained from a parallel execution on a desktop server like that targeted by our software. Although we will show that the parallelization of the framework and stages using OpenMP [10] is quite natural, we note that this is only possible because of the careful organization of the complete HPG-aligner mapping pipeline, specifically, the design of clean procedural interfaces and specialized shared data structures.

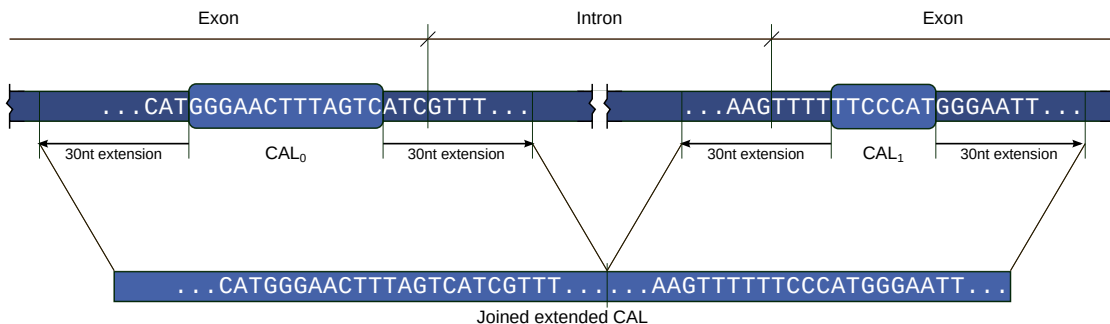


Figure 4: A joined extended CAL obtained by joining two extended CALs that are close to each other.

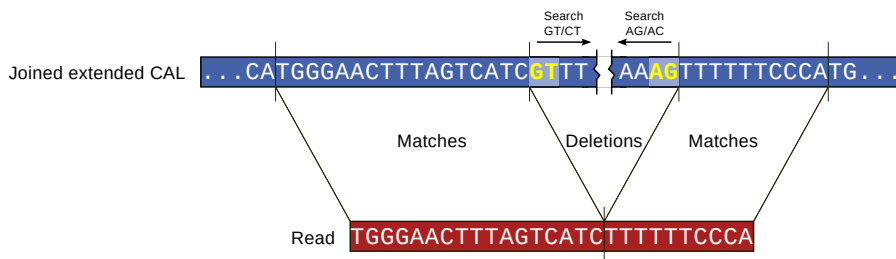


Figure 5: Splice junction detection.

3.1 General parallel framework

Listing 1 illustrates the parallelization of the pipelined HPG-aligner mapper using OpenMP. The organization of the algorithm into 6 independent stages (see Figure 1), connected via synchronization buffers, allows us to employ the OpenMP `sections` construct, with one thread dedicated to run each one of the stages, in principle yielding an overlapped (and, therefore, parallel) execution; see Figure 6 (top). For simplicity, we do not include certain details specific to the pipeline operation. For example, condition variables are employed in the actual implementation to synchronize consecutive stages, forcing the producer/consumer to stop when the shared queue is full/empty. Also, the operation of one particular stage is terminated when its input queue is empty and the previous stage indicates that it will produce no further new items (batches).

3.2 Stages A and F: Read Data and Write Results

These stages stream the data between the disk and the pipeline in batches of reads. They both proceed sequentially, as no attempt is made within each one of these stages to read/write multiple batches from/to disk simultaneously.

Listing 2 shows a simplified version of the process performed within these stages. Note how the procedure for stage A moves batches from the input file `FASTQ_file` to the “output” `Read_queue`, till the end of the file is detected. At that point, this stage notifies the following one that it will not produce new batches by setting `AB_pending_work` to `FALSE`.

The code for stage F performs the opposite process,

moving data from the `SWA_queue` to the file containing the mapping information, `BAM_file`, till there is no more `EF_pending_work` (notified by the previous stage) and the “input” `SWA_queue` is empty.

3.3 Stages B and C: Processing reads within a batch in parallel

Given a batch of reads, these two stages exploit that any two reads can be processed completely independently. Thus, in stage B we dedicate `nt_BWT` OpenMP threads to concurrently apply the BWT-based algorithm (with up to one EID) to process the reads of a batch (nested parallelism), with a straight-forward implementation that simply adds a loop-parallel OpenMP directive to the serial code; see the sample code in Listing 3. Termination is detected using the variable `AB_pending_work` (set by the previous stage) and the test on the contents of the `Read_queue`. Furthermore, detection of termination is notified to the subsequent stage by setting `BC_pending_work` to `FALSE` upon completion.

Note that each batch usually consists of 200 reads and, therefore, given the moderate number of cores available in current desktop servers, there exists a significant amount of concurrency per batch. Also, no special care is needed during the concurrent access to the data structure containing the batch of reads, as each thread will only modify the registers corresponding to a distinct read and, therefore, no race conditions are possible.

Similar comments apply to the search of regions performed in stage C: a simple OpenMP-based implementation suffices to exploit nested parallelism; and coordination with previous and subsequent stage is performed in an analogous manner, so that no race conditions

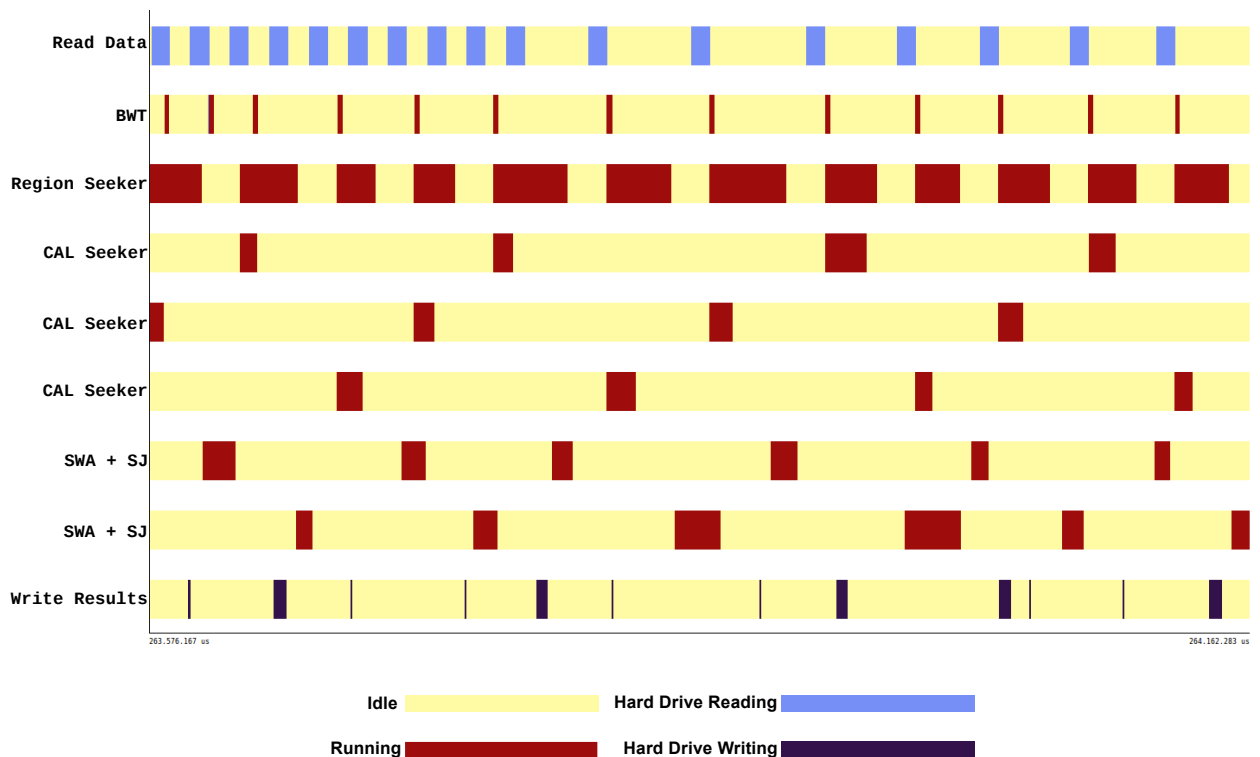
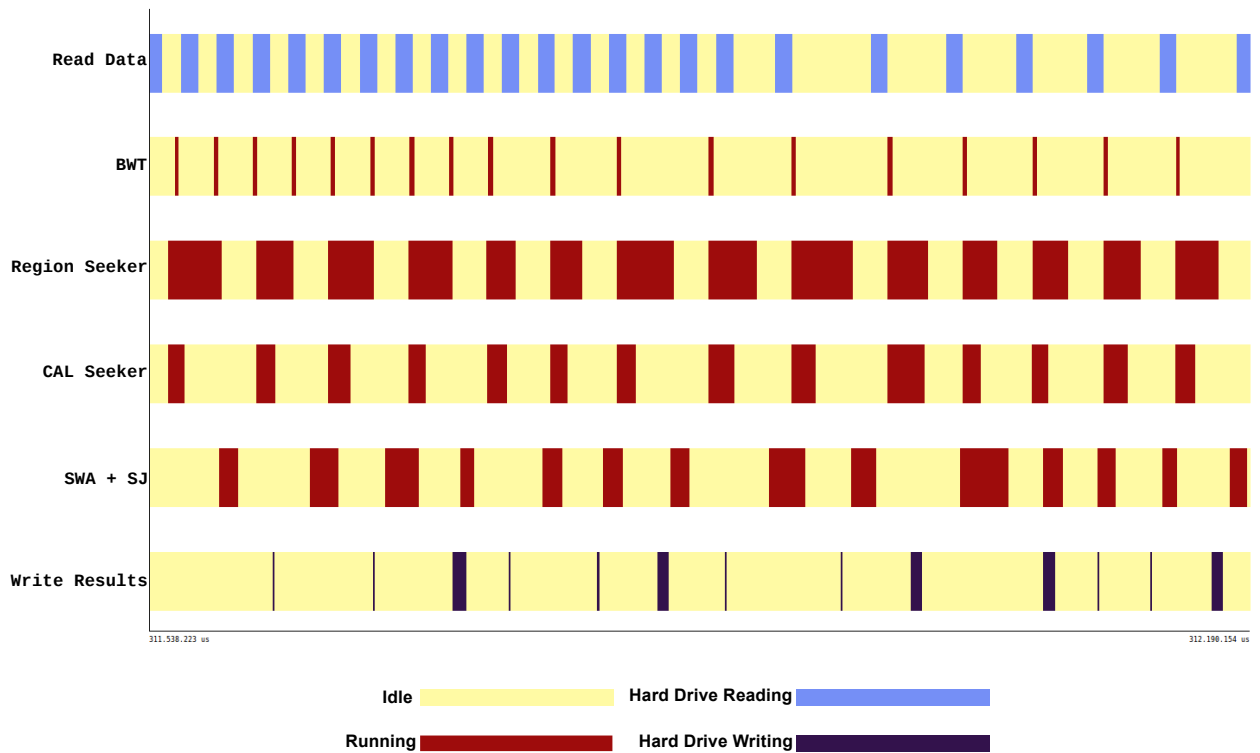


Figure 6: Traces of a pipelined execution of the mapper exploiting inter-stage concurrency (top) and both inter- and intra-stage concurrency (bottom). In the first case, a single thread is employed for each one of the pipeline stages: Read data, BWT, Region seeker, CAL seeker, SWA+SJ, and Write Results. The execution thus yields an interleaved execution with, e.g., I/O from/to disk proceeding in parallel with the other stages. The second case goes one step further in the exploitation of concurrency, employing, in this particular example, 3 threads for the CAL seeker and 2 for the SWA+SJ. The net result is that now several batches can be processed in parallel by different threads, even in the same stage.

Listing 1: Simplified version of pipelined framework parallelized using OpenMP.

```

1 #define num_stages    6
2 int AB_pending_work = TRUE,
3     BC_pending_work = TRUE,
4     CE_pending_work = TRUE,
5     EF_pending_work = TRUE;
6
7 #pragma omp parallel sections num_threads( num_stages ) {
8     #pragma omp section {
9         A_Read_Data( FASTQ_file, Read_queue );           // Read batches from FASTQ
10    }
11    #pragma omp section {
12        B_BWT( Read_queue, BWT_queue );                 // Apply the BWT
13    }
14    #pragma omp section {
15        C_Region_Seeker( BWT_queue, Region_queue );     // Apply Region seeker
16    }
17    #pragma omp section {
18        D_CAL_Seeker( Region_queue, CAL_queue );        // Apply CAL seeker
19    }
20    #pragma omp section {
21        E_SWA_Splice_Junctions( CAL_queue, SWA_queue ); // Apply SWA and
22                                                    // detect splice jcts
23        E_Write_Splice_Junctions( BED_file );          // Write results onto BAM
24    }
25    #pragma omp section {
26        F_Write_Data( SWA_queue, BAM_file );            // Write results onto BAM
27    }
28 }

```

Listing 2: Simplified version of serial reads and writes of batches within stages *A* and *F* respectively using OpenMP.

```

1 void A_Read_Data( FASTQ_file_t FASTQ_file, Read_queue_t Read_queue ) {
2     while ( !end_file( FASTQ_file ) ) {
3         A_Read_Batch( FASTQ_file, Batch ); // Read a single batch from
4         A_Write_Batch( Read_queue, Batch ); // FASTQ file onto Read_queue
5     }
6     AB_pending_work = FALSE;
7 }
8
9 void F_Write_Data( SWA_queue_t SWA_queue, BAM_file_t BAM_file ) {
10    while ( ( EF_pending_work ) OR ( !empty_queue( SWA_queue ) ) ) {
11        F_Read_Batch( SWA_queue, Batch ); // Write a single batch from SWA_queue
12        F_Write_Batch( BAM_file, Batch ); // onto BAM file
13    }
14 }

```

Listing 3: Simplified version of parallel processing of reads within stages *B* and *C* using OpenMP.

```

1 #define nt_BWT          ... // User-defined parameter
2 #define nt_Region_Seeker ... // User-defined parameter
3
4 void B_BWT( Read_queue_t Read_queue, BWT_queue_t BWT_queue ) {
5     while ( ( AB_pending_work ) OR ( !empty_queue( Read_queue ) ) ) {
6         B_BWT_Read( Read_queue, Batch );
7         #pragma omp parallel for num_threads( nt_BWT ) {
8             for ( i = 0; i < Batch.n_reads; i++ ) // Loop over all reads
9                 B_BWT_Single_Read( Batch.read[ i ] ); // Apply the BWT to the i-th read
10        }
11        B_BWT_Write( BWT_queue, Batch );
12    }
13    BC_pending_work = FALSE;
14 }
15
16 void C_Region_Seeker( BWT_queue_t BWT_queue, Region_queue_t Region_queue ) {
17     while ( ( BC_pending_work ) OR ( !empty_queue( BWT_queue ) ) ) {
18         C_Region_Read( BWT_queue, Batch );
19         #pragma omp parallel for num_threads( nt_Region_Seeker ) {
20             for ( i = 0; i < Batch.n_reads; i++ ) // Loop over all reads
21                 C_Region_Single_Read( Batch.read[ i ] ); // Apply Region seeker
22                                     // to the i-th read
23         }
24         C_Region_Write( Region_queue, Batch );
25     }
26     CD_pending_work = FALSE;
27 }

```

can result from the concurrent accesses to the data structures. However, note that now the degree of concurrency within a batch of reads is in general more reduced, as this stage only processes unmapped reads from the previous stage.

3.4 Stages *D* and *E*: Processing batches of reads in parallel

These stages exploit the independence among the information contained in the batches to process them concurrently (nested parallelism), with `nt_CAL_Seeker` and `nt_SWA_Splice_Junctions` threads (for stages *D* and *E*, respectively), using the `parallel` OpenMP directive. The degree of parallelism available at each one of these stages depends on the throughput of the previous stage. For example, provided stage *C* processes batches at sufficient speed, inserting these results onto the `Region_queue`, stage *D* will receive a constant flux of inputs, enough to feed the computational resources (threads) dedicated to search the CALs. Note again that the autonomy of the batches ensure that no special mechanism is necessary to avoid race conditions.

4 Experimental Results

The experiments reported in the next three subsections were performed on a platform equipped with four AMD

Opteron 6276 processors at 2.3 GHz, with 16 cores each (64 cores in total), and 64 Gbytes of RAM. This is a ccNUMA (cache-coherent non-uniform memory access) architecture where each processor has its own memory controller and local memory, and exchanges information with other processors via the HyperTransport interconnect.

In the following subsections we only study the parallelism of stages *B–E*. Due to its (intra-stage) sequential nature, stages *A* and *F* are executed by a single thread each. Independent experiments proved that the runtime of these two stages is negligible and, furthermore, their execution can be overlapped with the rest of the stages so that they exert a minor impact on the performance of the full pipeline.

4.1 Benchmarks

The experimental evaluation of the aligner is performed using simulated single-end datasets with 2 million reads of 100 and 250 nts. The former length is representative of recent RNA-seq while, with the dropping costs of this technology, reads of longer dimension (e.g., 250 nts) are becoming mainstream. Two scenarios were designed for variabilities (ε) of 0.1% and 1% of mismatches, with 30% of them being insertions/deletions. Hereafter, we will refer to the four benchmark test cases as τ_1 (100 nts, $\varepsilon = 0.1\%$), τ_2 (100 nts, $\varepsilon = 1\%$), τ_3 (250 nts, $\varepsilon = 0.1\%$), and τ_4 (250 nts, $\varepsilon = 1\%$). Simulations were carried out with the `dwgsim` program, from the SAM tools [13], setting the appropriate values for `n` (maximum number of Ns allowed in a given

Listing 4: Simplified version of parallel processing of batches within stages D and E using OpenMP.

```

1 #define nt_CAL_Seeker          ... // User-defined parameter
2 #define nt_SWA_Splice_Junctions ... // User-defined parameter
3
4 void D_CAL_Seeker( Region_queue_t Region_queue, CAL_queue_t CAL_queue ) {
5     #pragma omp parallel private( Batch ) num_threads( nt_CAL_Seeker ) {
6         while ( ( CD_pending_work ) OR ( !empty_queue( Region_queue ) ) ) {
7             D_CAL_Seeker_Read( Region_queue, Batch );
8             D_CAL_Seeker(          Batch ); // Apply CAL seeker to all reads
9             D_CAL_Seeker_Write( CAL_queue, Batch ); // within the batch
10        }
11    }
12    DE_pending_work = FALSE;
13 }
14
15 void E_SWA_Splice_Junctions( CAL_queue_t CAL_queue, SWA_queue_t SWA_queue ) {
16     #pragma omp parallel private( Batch ) num_threads( nt_SWA_Splice_Junctions ) {
17         while ( ( DE_pending_work ) OR ( !empty_queue( CAL_queue ) ) ) {
18             E_SWA_Splice_Junctions_Read( CAL_queue, Batch );
19             E_SWA_Splice_Junctions(          Batch ); // Apply SWA/detect splice
20             E_SWA_Splice_Junctions_Write( SWA_queue, Batch ); // jcts to/in all reads
21                                     // within the batch
22        }
23    }
24    EF_pending_work = FALSE;
25 }

```

read), r (rate of mutations), and c (mean coverage across available positions).

4.2 Intra-stage concurrency

Our first study investigates the parallelism and scalability of the algorithms employed in stages B – E . Consider one of this stages, e.g., D . In order to avoid interferences in this evaluation, we initially block (the threads in charge of executing) stage D and run all stages of the pipeline prior to it (i.e., A – C) to completion, so that the Region queue, between C and D (see Figure 1), is filled with the same data that the pipelined execution would produce for each test case. We next block the stages after D (i.e., E and F) and let this one operate in isolation, with a variable number of threads executing it. The results thus illustrate the strong scalability of the algorithm employed in the stage in the ideal case when other stages are disabled and, therefore, no memory conflicts occur with these other stages.

Table 1 reports the execution time of stages B – E and test cases T1–T4 when up to 20 threads are employed for the execution. Figure 7 displays the corresponding speed-ups (obtained dividing the serial time, i.e., with one thread, by the parallel time). The first aspect to note from these results is the much higher cost of stage C for the T1 and T2 cases, and the higher cost of stage E for the remaining two cases when a single thread is employed.

On the other hand, there is a similar parallel behaviour of the algorithms for all four benchmarks, with the BWT-based algorithm (stage B) showing the worst scalability, much below those of the algorithms employed in the other

three stages. In principle, stage B exhibits a perfect degree of parallelism: all reads within a batch are independent and, therefore, they can be processed concurrently. To leverage this, in our implementation of this stage each thread extracts a read from the input queue, processes it, and inserts the result in the BWT queue. However, the BWT presents an irregular access pattern to the data as well as a low computation-communication (memory transfers) ratio. Furthermore, the implementation operates on a vector that does not fit into the cache memory, rendering the BWT-based algorithm a memory-bounded process that is intrinsically limited by the bandwidth of the interconnect to memory. Stage C also employs the same algorithm, though this time it does so to map seeds instead of complete reads. This partially explains the superior execution time of this stage as each read that remained unmapped from the previous stage is now split into a collection of seeds to be mapped. On the other hand, it seems that the fact that the seeds of a read will likely map in nearby areas of the genome helps in reducing the amount of references to non-cached data, resulting in a higher speed-up for this stage. Finally, stages D and E show a good linear scalability that grows steadily with the number of threads.

4.3 Inter- and Intra-stage concurrency

Armed with the previous results, we now study the performance of the full pipeline. Since the target platform has 64 cores, we could distribute (up to) an analogous number of threads arbitrarily among the different stages of the pipeline, reserving two cores/threads for the execution of

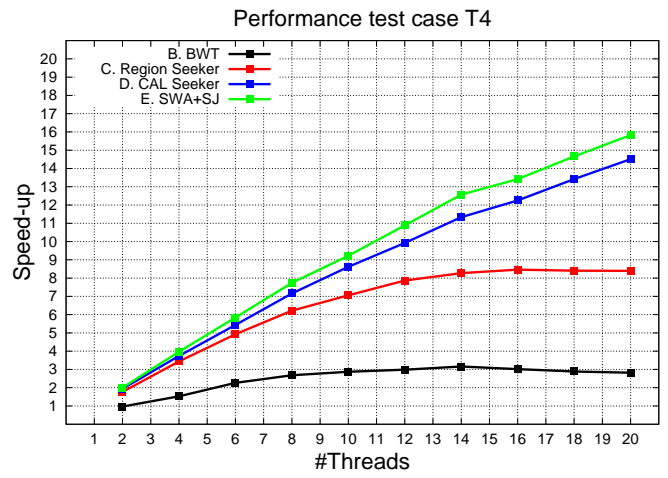
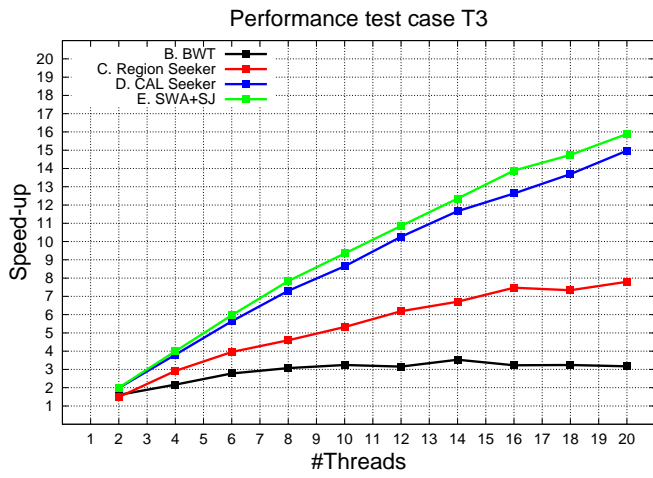
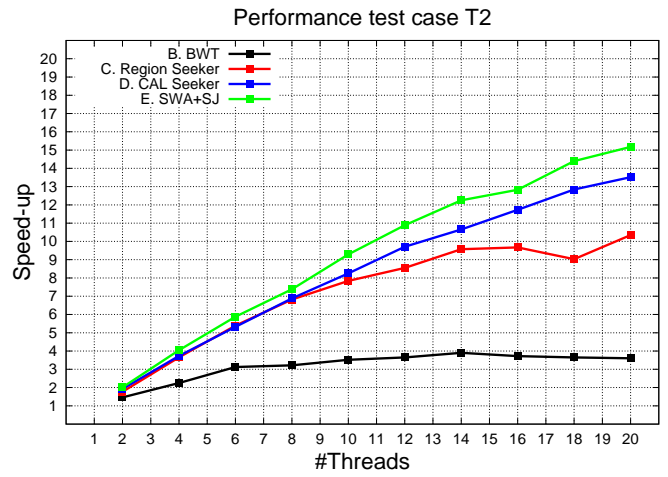
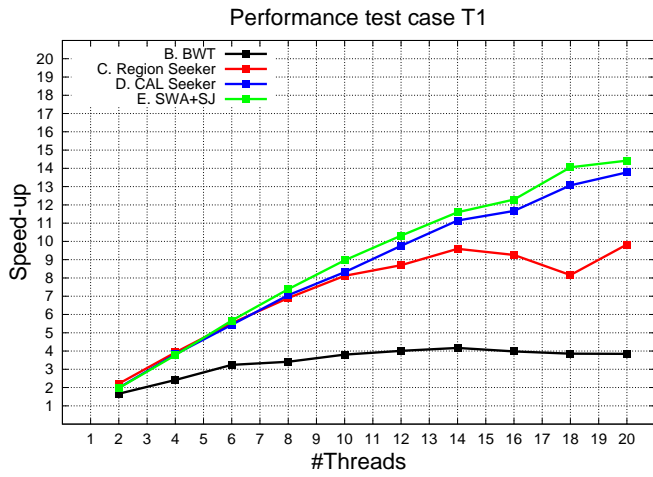


Figure 7: Speed-ups of stages $B-E$ for the four test cases.

Table 1: Execution time (in s.) of stages B – E for the four test cases.

(a) Test case T1: 100 nts, $\varepsilon = 0.1\%$.					(b) Test case T2: 100 nts, $\varepsilon = 1\%$.				
Threads	Time per stage				Threads	Time per stage			
	B	C	D	E		B	C	D	E
1	38.58	562.80	219.79	318.02	1	32.42	615.99	243.33	361.26
2	23.20	254.14	110.53	161.19	2	22.20	347.88	126.31	179.54
4	16.00	143.42	57.56	84.30	4	14.43	168.50	65.24	89.35
6	11.89	101.87	40.45	56.12	6	10.37	114.26	45.71	61.46
8	11.31	81.52	31.15	43.07	8	10.08	90.33	35.36	48.95
10	10.14	69.34	26.42	35.46	10	9.21	78.58	29.49	38.88
12	9.62	64.69	22.52	30.83	12	8.88	72.06	25.06	33.19
14	9.26	58.65	19.72	27.43	14	8.31	64.36	22.84	29.49
16	9.70	60.78	18.84	25.87	16	8.71	63.68	20.74	28.17
18	10.01	69.00	16.82	22.62	18	8.89	68.23	18.95	25.09
20	10.04	57.25	15.95	22.05	20	9.00	59.55	18.00	23.81

(c) Test case T3: 250 nts, $\varepsilon = 0.1\%$.					(d) Test case T4: 250 nts, $\varepsilon = 1\%$.				
Threads	Time per stage				Threads	Time per stage			
	B	C	D	E		B	C	D	E
1	37.07	1,545.78	730.98	2,198.11	1	36.67	1,872.21	711.24	2,149.98
2	23.05	1,039.40	367.63	1,098.15	2	37.89	1,058.06	366.99	1,074.69
4	17.11	529.66	192.09	550.30	4	24.00	544.68	190.43	541.59
6	13.34	391.12	129.66	368.46	6	16.20	380.14	130.88	367.99
8	12.06	336.35	100.11	280.41	8	13.68	301.08	99.37	277.76
10	11.44	290.42	84.55	235.23	10	12.77	265.31	82.56	233.05
12	11.75	249.79	71.23	202.54	12	12.28	238.11	71.67	197.50
14	10.50	230.41	62.66	177.94	14	11.60	226.34	62.75	171.05
16	11.49	206.89	57.87	158.29	16	12.16	221.27	58.05	160.21
18	11.43	210.77	53.39	149.09	18	12.71	222.73	53.00	146.68
20	11.69	198.17	48.82	138.32	20	13.01	223.02	49.01	135.84

stages A and F (I/O from/to disk, respectively). However, the following two observations guided our choices.

First, the performance of a pipeline is limited by the slowest stage so that it is convenient to assign the throughput of resources carefully to equilibrate the execution time of the stages. In particular, the execution times in Table 1 clearly ask for the application of a higher number of threads to the execution of stages C – E than to B . Depending on the test case, it is more convenient to dedicate more threads to stage C or E , though in any case these numbers should be superior than to those dedicated to D . Note that these values are set through constants `nt_BWT`, `nt_Region_Seeker...` in our codes.

The second observation is that the maximum number of threads that it is convenient to dedicate to certain stages is limited. For example, the analysis of the results Figure 7 reveals that assigning more than 4–6 threads for stage B or, depending on the case, more than 12–16 threads for stage C , is useless.

Following these two principles, let us examine the performance of the parallel execution of the pipeline. The complete results from this experiment are collected in Table 2 and summarized in Figure 8. The total time includes also I/O from/to disk so that the actual number of threads employed in this experiment is that showed in the corresponding column plus the (two) I/O threads. The execu-

tion times per stage only reflect the period of time when the thread of the corresponding stage is active, processing data, but excludes the period that the thread is idle, e.g., waiting because there is no work in the input queue.

Consider, e.g., the results for benchmark T1 in Table 2. The first row of this table, labelled as “Sequential version”, reports the times measured in a sequential execution of the pipeline —i.e., no overlapping— (recall Table 1), and the total time resulting from that. (For simplicity, the cost of I/O is not included in the serial execution time.) The second row corresponds to an overlapped execution of the pipeline, with one thread per stage (4 for B – E). Compared with the runtime per stage of the serial case, the execution time of all stages is increased, likely due to memory conflicts but also to the overheads of the pipeline (e.g., initial and final latencies). However, the overlapped execution renders a lower total time (617.34s for the pipelined execution vs 1,139.20s for the serial one), which basically agrees with that of the execution time of the slowest stage (610.39s for stage C), showing a remarkable degree of overlapping.

Given the outcome of this initial experiment, it is natural to start by assigning a higher number of threads to the execution of stage C . Consider now the third row of the table, which reports the execution time when 7 threads are employed in the computation, 4 of them for stage C . This configuration reduces the execution time of stage C from

610.39s to 168.32s, and the total time to 350.04s, which was to be expected because now the bottleneck is shifted to stage *E*. As a side effect, the time required for stage *D* is also significantly reduced, but with no impact on the total time.

The following two configurations employ 8 threads, further reducing the total execution time, but with a different distribution: 1+3+1+3 and 1+4+1+2, with the first one obtaining slightly better results (312.33s vs 314.04s). By increasing the number of threads, while distributing them with care among the different stages, we can still reduce the execution time up to 62 threads (remember that the remaining 2 threads are necessary for I/O). The best configuration in this case is 10+20+16+16 and results in a balanced execution time of stages *C* and *D*, which exhibit now the longest execution times. Although, in principle, we could shift some threads from stages *B* and *E* in an attempt to accelerate stage *C*, according to the experiments reported in Table 1 and the top left plot of Figure 7, we cannot expect much improvement from that. Thus, any further effort to accelerate the pipeline, by shifting threads among stages, is useless given the bottleneck that the lack of further concurrency of stage *C* represents at this point. A similar analysis holds for the remaining three test cases.

Figure 8 shows the speed-up of the full pipeline (serial time divided by parallel time) for up to 62+2 threads. These results show performance improvements in the range of 7.9–9.0 for 16+2 threads, 9.6–10.6 for 27+2 threads, and 11.4–16.0 using 62+2 threads. For benchmarks T1–T2, for example, this represents a reduction of the mapping process from around 19–20 minutes to about 1.5 minutes. For benchmarks T3–T4, on the other hand, the reduction is from approximately 1 hour and 15–20 minutes to only about 5 minutes.

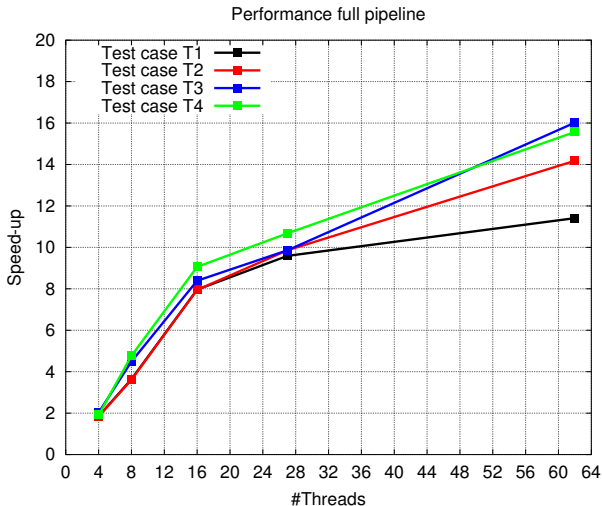


Figure 8: Speed-up of the full pipeline for the four test cases.

4.4 Comparison with TopHat 2

We have compared HPG-aligner to the most extensively used RNA-seq mapper, TopHat 2, combined with both Bowtie and Bowtie 2 using the four test cases, on a platform

with 2 Intel Xeon E5645 processors at 2.40 GHz (six cores per processor), and 48 Gbytes of RAM (ccNUMA). To obtain the following results, all the RNA-seq software, including our HPG-aligner, was executed with the default input parameters, using all cores of the platform. For that purpose, we set the flag $p=12$ for TopHat 2 while we employed 1+6+2+3 threads for the pipelined aligner. The results in Table 3 show that HPG-aligner is consistently over six times faster than TopHat 2 combined with Bowtie 2. In addition, the sensitivity of the proposed aligner, measured as the percentage of reads that were correctly mapped, clearly outperforms that of TopHat 2 with both Bowtie and Bowtie 2. When the read length grows, this difference in sensitivity is even more acute, as HPG-aligner increases its sensitivity while that of TopHat 2 drops. Similar results were obtained when the aligners were applied to real datasets.

5 Conclusions

We have introduced a pipeline for RNA sequencing, the HPG-aligner, that efficiently accommodates variable levels of hardware concurrency in current multicore technology, enabling fast mapping onto a reference genome, with a cost that linearly depends on the number and length of the RNA fragments. Our solution leverages a well-known principle, that of “*making the common case fast*”, to apply a variant of BWT in order to map those reads with at most 1 EID in a short period of time. (Note that the reliability of current NGS technology ensures that this part constitutes a large fraction of the total.) After this initial stage, mapping failures are expected to be mostly due to reads with more than 1 EID or, alternatively, reads that span over two or more exons. To tackle both cases, we proceed by dividing the reads into a collection of short seeds, which are next mapped using the fast BWT (again), yielding a collection of CALs in the reference genome. This information is finally passed to the accurate SWA that, under these conditions, turns most of the previous failures into successful mappings at a low cost.

Experiments on a server with a high number of cores reveal the parallel efficiency of the HPG-aligner pipeline, which is ultimately constrained by the serial performance of the expensive Region seeker. Future work will therefore aim at ameliorating part of the bottleneck imposed by this stage, possibly by further subdividing it into new (sub-)stages or shifting part of its cost towards neighboring stages.

Acknowledgments

The researchers from the Universidad Jaume I (UJI) were supported by project TIN2011-23283 and FEDER.

References

- [1] M. Garber, M. G. Grabherr, M. Guttman, and C. Trapnell, “Computational methods for transcriptome annotation and quantification using RNA-seq,” *Nature methods*, vol. 8, pp. 469–477, 2011.

Table 2: Execution time (in s.) of stages B – E when the full pipeline is in operation for the four test cases.

(a) Test case T1: 100 nts, $\varepsilon = 0.1\%$.

Threads per stage				Total threads	Time per stage				Total time
B	C	D	E		B	C	D	E	
Sequential version				1	38.58	562.80	219.79	318.02	1,139.20
1	1	1	1	4	51.81	610.39	284.37	335.97	617.34
1	4	1	1	7	51.86	168.63	305.81	338.55	350.04
1	3	1	3	8	53.49	228.63	300.93	119.59	312.33
1	4	1	2	8	55.28	181.01	302.40	178.37	314.06
1	6	2	4	13	59.12	128.89	175.30	96.31	188.54
1	7	3	5	16	59.12	121.24	129.44	84.27	143.08
1	16	4	6	27	70.52	85.35	104.60	73.84	118.77
10	20	16	16	62	29.44	84.11	84.20	30.06	99.79
14	16	16	16	62	25.64	86.50	86.58	27.83	101.33

(b) Test case T2: 100 nts, $\varepsilon = 1\%$.

Threads per stage				Total threads	Time per stage				Total time
B	C	D	E		B	C	D	E	
Sequential version				1	32.42	615.99	243.33	361.26	1,253.00
1	1	1	1	4	45.38	675.84	314.04	368.31	682.56
1	4	1	1	7	47.92	210.29	340.54	370.18	386.65
1	3	1	3	8	48.60	263.42	336.08	132.42	347.19
1	4	1	2	8	48.02	196.94	335.60	195.06	346.70
1	6	2	4	13	53.00	149.69	194.00	108.79	207.30
1	7	3	5	16	54.64	130.18	143.52	90.47	157.58
1	16	4	6	27	60.91	77.58	112.33	76.94	127.06
10	20	16	16	62	27.01	72.00	28.86	30.82	88.35
14	16	16	16	62	23.83	79.74	27.31	30.82	95.30

(c) Test case T3: 250 nts, $\varepsilon = 0.1\%$.

Threads per stage				Total threads	Time per stage				Total time
B	C	D	E		B	C	D	E	
Sequential version				1	37.07	1,545.78	730.98	2,198.11	4,511.90
1	1	1	1	4	59.24	1,894.40	1,012.06	2,210.04	2,213.96
1	4	1	1	7	60.57	555.15	1,036.71	2,239.92	2,243.22
1	3	1	3	8	56.58	708.99	996.13	791.78	1,005.60
1	4	1	2	8	59.25	536.20	1,055.92	1,151.74	1,165.00
1	6	2	4	13	55.58	440.36	614.39	624.30	653.12
1	7	3	5	16	58.68	409.53	463.20	522.25	538.09
1	16	4	6	27	74.69	225.18	343.19	439.64	457.39
10	20	16	16	62	36.49	261.19	79.91	203.42	281.58
14	16	16	16	62	43.25	286.86	73.86	208.09	307.00

(d) Test case T4: 250 nts, $\varepsilon = 1\%$.

Threads per stage				Total threads	Time per stage				Total time
B	C	D	E		B	C	D	E	
Sequential version				1	36.67	1,872.21	711.24	2,149.98	4,770.10
1	1	1	1	4	46.42	2,403.74	867.36	2,169.78	2,495.65
1	4	1	1	7	54.36	648.26	1,052.56	2,209.51	2,274.34
1	3	1	3	8	51.54	844.20	988.80	809.24	999.75
1	4	1	2	8	51.76	633.85	1,024.40	1,125.76	1,136.65
1	6	2	4	13	51.75	471.66	595.90	653.56	671.46
1	7	3	5	16	54.85	416.75	456.66	508.98	526.43
1	16	4	6	27	65.80	256.04	341.97	428.24	446.64
10	20	16	16	62	37.62	285.48	82.72	211.68	306.29
14	16	16	16	62	40.06	313.45	73.51	216.00	333.45

Table 3: Comparison of sensitivity (in %) and runtime (in minutes) of three RNA-seq aligners. In those cases labelled as “NA”, the program was stopped after three days in execution, with no results produced at that point.

	HPG-aligner		TopHat 2 + Bowtie		TopHat 2 + Bowtie 2	
	Sensitivity	Time	Sensitivity	Time	Sensitivity	Time
T1	97.15	2.41	62.47	23.71	62.09	20.13
T2	95.88	2.66	46.78	21.65	47.64	25.05
T3	97.32	14.76	NA	NA	NA	NA
T4	97.15	14.52	NA	NA	NA	NA

- [2] B. Langmead, C. Trapnell, M. Pop, and S. L. Salzberg, “Ultrafast and memory-efficient alignment of short DNA sequences to the human genome,” *Genome biology*, vol. 10, no. 3, p. R25, 2009.
- [3] H. Li and N. Homer, “A survey of sequence alignment algorithms for next-generation sequencing,” *Brief Bioinform*, vol. 11, pp. 473–483, 2010.
- [4] D. Adjeroh, T. C. Bell, and A. Mukherjee, *The Burrows-Wheeler Transform: Data Compression, Suffix Arrays, and Pattern matching*. Springer, 2008.
- [5] R. Li, C. Yu, Y. Li, T.-W. Lam, S.-M. Yiu, K. Kristiansen, and J. Wang, “Soap2: an improved ultrafast tool for short read alignment,” *Bioinformatics*, vol. 25, no. 1966–1967, 2009.
- [6] L. Heng and D. Richard, “Fast and accurate long-read alignment with burrows-wheeler transform,” *Bioinformatics*, vol. 26, no. 589–595, 2010.
- [7] C. Trapnell, L. Pachter, and S. L. Salzberg, “TopHat: discovering splice junctions with RNA-seq,” *Bioinformatics*, vol. 25, no. 9, pp. 1105–1111, 2009.
- [8] L. Ben and S. Steven L, “Fast gapped-read alignment with Bowtie 2,” *Nature methods*, vol. 9, no. 4, pp. 357–359, 2012.
- [9] T. F. Smith and M. S. Waterman, “Identification of common molecular subsequences,” *J. Mol. Biol.*, vol. 147, pp. 195–197, 1981.
- [10] OpenMP Architecture Review Board, “OpenMP web site,” <http://www.openmp.org/>.
- [11] P. J. A. Cock, C. J. Fields, N. Goto, M. L. Heuer, and P. M. Rice, “The Sanger FASTQ file format for sequences with quality scores, and the Solexa/Illumina FASTQ variants,” *Nucleic Acids Research*, vol. 38, no. 6, pp. 1767–1771, 2010.
- [12] UCSC Genome Bioinformatics, “BED format,” <http://genome.ucsc.edu/FAQ/FAQformat.html#format1>.
- [13] SAMtools, “BAM/SAM API documentation,” <http://samtools.sourceforge.net/>.
- [14] J. L. Hennessy and D. A. Patterson, *Computer Architecture: A Quantitative Approach*, 5th ed. San Francisco: Morgan Kaufmann Pub., 2012.